

## Fractionally-Spaced Equalizer Based on High-Order Statistics in Nonlinear Fiber Optics

Koike-Akino, T.; Duan, C.; Parsons, K.; Kojima, K.

TR2012-004 January 2012

### Abstract

Fiber non-linearity has become a major limiting factor to realize ultra-high-speed optical communications. We propose a fractionally-spaced equalizer which exploits a trained high-order statistics (mean, variance, skewness, etc.) to deal with data-pattern dependent nonlinear impairments in fiber-optic communications. The computer simulation reveals that the proposed 3-tap equalizer improves Q-factor by more than 2 dB for long-haul transmissions of 5,230km distance and 40 Gbps data rate. We also demonstrate that the joint use of a digital back propagation (DBP) and the proposed equalizer offers an additional 12 dB performance improvement due to the channel shortening gain. A performance in beyond 100 Gbps high-speed transmissions is evaluated as well.

*IEICE Optical Communication Systems (OCS)*

This work may not be copied or reproduced in whole or in part for any commercial purpose. Permission to copy in whole or in part without payment of fee is granted for nonprofit educational and research purposes provided that all such whole or partial copies include the following: a notice that such copying is by permission of Mitsubishi Electric Research Laboratories, Inc.; an acknowledgment of the authors and individual contributions to the work; and all applicable portions of the copyright notice. Copying, reproduction, or republishing for any other purpose shall require a license with payment of fee to Mitsubishi Electric Research Laboratories, Inc. All rights reserved.



# 非線形光ファイバにおける高次統計量を利用した分数間隔等化方式

秋濃 俊昭<sup>†</sup> 段 春傑<sup>†</sup> Kieran PARSONS<sup>†</sup> 小島 啓介<sup>†</sup>

吉田 剛<sup>††</sup> 杉原 隆嗣<sup>††</sup> 水落 隆司<sup>††</sup>

<sup>†</sup> Mitsubishi Electric Research Labs. (MERL) 201 Broadway, Cambridge, MA 02139, USA

<sup>††</sup> 三菱電機株式会社 情報技術総合研究所 〒247-8501 神奈川県鎌倉市大船 5-1-1

E-mail: <sup>†</sup>{koike,duan,parsons,kojima}@merl.com,

<sup>††</sup>{Yoshida.Tsuyoshi,Sugihara.Takashi,Mizuochi.Takashi}@ah.MitsubishiElectric.co.jp

あらまし 光ファイバ通信において超高速通信を実現するには非線形歪を補償することが重要である。非線形歪は送信信号データに依存することが知られており、本稿ではこれを利用した等化方式を提案している。本方式は光ファイバ入出力応答の多次元高次統計量（平均・分散・歪度など）を適応的に学習し、データ依存のある非線形歪を効率よく補償する分数間隔等化を適用している。提案方式の利用により 40 Gbps の伝送速度・5,230 km の伝送距離において 2 dB 以上の特性改善効果が得られることを計算機シミュレーションで明らかにする。また、デジタル後方伝搬を等化器の前段に用いることで伝搬路応答のメモリ長を短縮し、1-2 dB のさらなる特性改善が可能であることを示す。また、100 Gbps 超の高速通信時における特性改善効果も議論する。

キーワード 光ファイバ、非線形歪補償、高次統計量、分数間隔等化、最尤推定、デジタル後方伝搬

## Fractionally-Spaced Equalizer Based on High-Order Statistics in Nonlinear Fiber Optics

Toshiaki KOIKE-AKINO<sup>†</sup>, Chunjie DUAN<sup>†</sup>, Kieran PARSONS<sup>†</sup>, Keisuke KOJIMA<sup>†</sup>,

Tsuyoshi YOSHIDA<sup>††</sup>, Takashi SUGIHARA<sup>††</sup>, and Takashi MIZUOCHI<sup>††</sup>

<sup>†</sup> Mitsubishi Electric Research Labs. (MERL) 201 Broadway, Cambridge, MA 02139, USA

<sup>††</sup> Information Technology R&D Center, Mitsubishi Electric Corporation 5-1-1 Ofuna, Kamakura, Kanagawa 247-8501, Japan

E-mail: <sup>†</sup>{koike,duan,parsons,kojima}@merl.com,

<sup>††</sup>{Yoshida.Tsuyoshi,Sugihara.Takashi,Mizuochi.Takashi}@ah.MitsubishiElectric.co.jp

**Abstract** Fiber nonlinearity has become a major limiting factor to realize ultra-high-speed optical communications. We propose a fractionally-spaced equalizer which exploits a trained high-order statistics (mean, variance, skewness, *etc.*) to deal with data-pattern dependent nonlinear impairments in fiber-optic communications. The computer simulation reveals that the proposed 3-tap equalizer improves Q-factor by more than 2 dB for long-haul transmissions of 5,230 km distance and 40 Gbps data rate. We also demonstrate that the joint use of a digital backpropagation (DBP) and the proposed equalizer offers an additional 1-2 dB performance improvement due to the channel shortening gain. A performance in beyond 100 Gbps high-speed transmissions is evaluated as well.

**Key words** Optical fiber, nonlinearity compensation, high-order statistics, fractionally-spaced equalizer, maximum-likelihood estimation, digital backpropagation

### 1. Introduction

Digital coherent optical transmissions have a potential to increase data rates with dual-polarized phase-shift key-

ing (DP-PSK) and quadrature-amplitude modulation (DP-QAM). However, fiber nonlinearity can significantly degrade the advantage of coherent transmission systems over conventional non-coherent transmission systems as such spectrally

efficient modulation formats require higher signal power which causes higher nonlinear distortion [1], [2]. Therefore, to mitigate fiber nonlinearity has been of great importance in optical communication researches.

Recently, it was shown that digital back-propagation (DBP) proposed in [3], [4] offers a substantial performance gain for nonlinear compensation. However, the DBP requires high-complexity processing based on split-step Fourier methods (SSFM). Although there exist several reduced-complexity methods [5] ~ [8], the performance is susceptible to the amplified spontaneous emission (ASE) noise and the polarization mode dispersion (PMD). Moreover, the SSFM parameters used in DBP should be manually adjusted to achieve the best performance in general.

We focus on an alternative method based on statistical sequence equalizers (SSE), studied in [9], [10], which mitigates data-pattern-dependent nonlinearity. In the scheme presented in [10], the first-order statistics (i.e., the mean of the the nonlinear distortion) is trained first for some possible data patterns, and the pattern matching is performed to equalize the nonlinearity. The statistical sequence equalizer achieves good performance with low complexity for short-memory channels, and could be combined with other methods including DBP and frequency-domain equalizer (FDE).

In this paper, we extend the original SSE in several directions: i) we propose the use of second-order statistics (i.e., not only mean but also covariance), ii) we adopt a fractionally-spaced signal processing, iii) we use an excess window size for pattern matching, and iv) we introduce a cascaded equalizer which employs a reduced-complexity DBP to shorten the channel memory in conjunction with a statistical equalizer to suppress the residual nonlinearity.

Through the computer simulations, we obtain more than 2dB improvement using the proposed equalizer for coherent optical communications with 40 Gbps non-return-to-zero (NRZ) DP-QPSK or differential QPSK (DP-DQPSK) signals after 5,230 km transmissions. The achieved performance is better than that of the DBP in low local dispersion channels, and is comparable to the DBP in high local dispersion channels. We also demonstrate that the joint use of DBP and SSE enjoys an additional 1–2dB gain. A performance improvement of the cascaded equalizer is evaluated for beyond 100 Gbps high-speed transmissions as well.

## 2. Nonlinear Equalizer

Fig. 1 shows the schematic of the proposed statistical sequence equalizer in coherent optical communications. The digital data  $s_k$  at the time instance  $k$  is transmitted through the nonlinear fiber by using the coherent optical transceiver. The received data may be first processed by several pre-

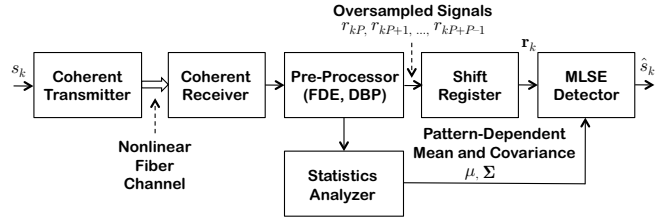


図 1 コヒーレント光通信システムにおける非線形歪の高次統計量を用いた分数間隔等化器 .

Fig. 1 Fractionally-spaced statistical sequence equalizer (FS-SSE) which exploits high-order statistics of nonlinearity distortion in coherent fiber-optic systems.

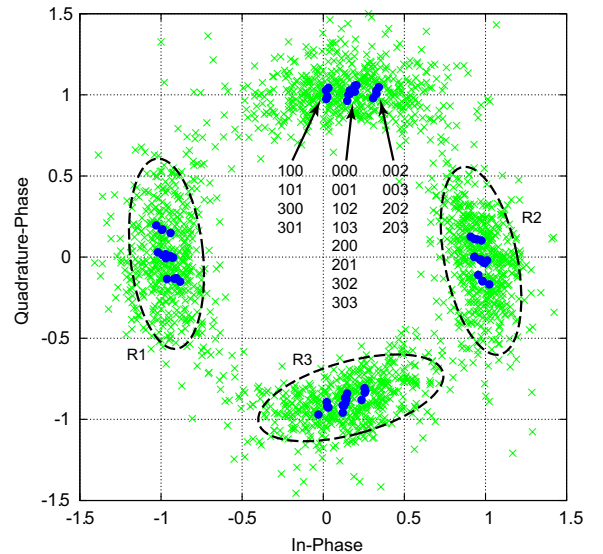


図 2 非線形歪のある受信 I-Q 信号例 (送信電力  $-4$  dBm, 波長  $1551$  nm, ファイバ長  $5,230$  km) .

Fig. 2 Examples of received I-Q constellation with nonlinear distortion (launching power:  $-4$  dBm, wavelength:  $1551$  nm, fiber distance:  $5,230$  km).

equalization units, including timing recovery, FDE for chromatic dispersion compensation, PMD compensation, DBP for nonlinear compensation, and so on. The pre-processed signal is fed into a shift register which accepts fractionally-spaced (or, oversampled) data. Those signals are also analyzed to obtain the statistics of the fiber nonlinearity. The oversampled data is then equalized by a maximum-likelihood sequence estimation (MLSE) detector which employs the Viterbi algorithm based on the fiber statistics.

### 2.1 Statistical Sequence Equalizer (SSE)

As discussed in [10], intra-channel nonlinear distortion highly depends on the transmitted data pattern. The statistical sequence equalizer (SSE) in [10] first acquires such data-pattern-dependent distortion characteristics by averaging the received sequence with training data or on-line learning process. The trained mean signals are then used to equalize the nonlinear distortion by searching for a pattern with the minimum Euclidean distance from the received sequence.

Fig. 2 illustrates an example of the received I-Q (In-phase/Quadrature-phase) constellations distorted by the fiber nonlinearity for a launching power of  $-4$  dBm over 5,230 km long-haul transmissions (corresponding to 8 dBQ with a 1-tap phase compensator). Here, we plot 4,000 sample-spaced receiving signals of a random DQPSK sequence. To show the data-pattern-dependent nonlinearity, we also present the averaged signal points of the  $k$ -th received signal  $\mathbb{E}[r_k]$  conditioned on the consecutive 3-symbol data pattern  $\mathbf{s}_k = [s_{k-1}, s_k, s_{k+1}]$ , where  $\mathbb{E}[\cdot]$  denotes the expectation. There are 64 points in the figure since the total number of the different data patterns is  $4^3 = 64$  from  $\mathbf{s}_k = [0, 0, 0]$  to  $[3, 3, 3]$  for a 3-tap data sequence. It can be seen from Fig. 2 that the mean of the received signal (e.g. for the data pattern  $[0, 0, 0]$ ) differs from that for another (e.g.  $[0, 0, 2]$ ). The SSE exploits such a data-pattern-dependent distortion to compensate the nonlinearity.

## 2.2 High-Order Statistics

In this paper, we propose the use of higher-order statistics (variance, skewness, *etc.*) in addition to the first-order statistics (mean) to mitigate residual nonlinear noise as well. As shown in Fig. 2, the residual (out-of-memory) nonlinear distortion performs as an effective noise which also depends on the data pattern; specifically, the distribution of the residual distortion around the region “R1” is different from that of the region “R3.” More importantly, the distribution is not circularly symmetric (i.e., ellipsoidal rather than circular).

To take the pattern-dependent residual nonlinearity into account properly, we introduce a model based on a circularly-asymmetric Gaussian distribution. We consider a window size of  $N$  receiving samples centered around the target transmission data to establish an empirical statistics. Let  $\mathbf{r}_k = [r_{k-\lfloor(N-1)/2\rfloor}, \dots, r_k, \dots, r_{k+\lfloor N/2\rfloor}]^T \in \mathbb{C}^N$  denote the received signal sequence in the shift register of window size  $N$ , where  $\lfloor \cdot \rfloor$ ,  $[\cdot]^T$ , and  $\mathbb{C}$  denote a floor function, a transpose operation, and a complex-number set, respectively. A statistics analyzer obtains the empirical mean vector and the covariance matrix of the received signals for each transmission data pattern  $\mathbf{s} = [s_{k-\lfloor(M-1)/2\rfloor}, \dots, s_k, \dots, s_{k+\lfloor M/2\rfloor}] \in \mathbb{N}^M$ , where  $\mathbb{N}$  denotes the natural number set (positive integers).

Letting  $\mathbf{s}$  be one of the  $4^M$  possible data patterns (for 4-ary data), the empirical mean vectors  $\boldsymbol{\mu}(\mathbf{s}) \in \mathbb{R}^{2N}$  and the covariance matrices  $\boldsymbol{\Sigma}(\mathbf{s}) \in \mathbb{R}^{2N \times 2N}$  are expressed as follows:

$$\boldsymbol{\mu}(\mathbf{s}) = \frac{1}{\mathcal{N}(\mathbf{s})} \sum_{j: \mathbf{s}_j = \mathbf{s}} \mathbf{r}'_j, \quad (1)$$

$$\boldsymbol{\Sigma}(\mathbf{s}) = \frac{1}{\mathcal{N}(\mathbf{s}) - 1} \sum_{j: \mathbf{s}_j = \mathbf{s}} (\mathbf{r}'_j - \boldsymbol{\mu}(\mathbf{s})) (\mathbf{r}'_j - \boldsymbol{\mu}(\mathbf{s}))^T, \quad (2)$$

where we define  $\mathbf{r}'_j \triangleq [\Re[\mathbf{r}_j^T], \Im[\mathbf{r}_j^T]]^T \in \mathbb{R}^{2N}$ . Here,  $\mathcal{N}(\mathbf{s})$  is the total number of occurrences that the data pattern  $\mathbf{s}$

appeared in the past. The notations  $\mathbb{R}$ ,  $\Re[\cdot]$  and  $\Im[\cdot]$  are a real-number set, the element-wise real part and imaginary part operations, respectively. The main reason to expand the complex-valued vector  $\mathbf{r}_j$  to a double-size real-valued vector  $\mathbf{r}'_j$  is to model the circular asymmetry illustrated in Fig. 2.

With the trained statistics, the expected likelihood of the received signals  $\mathbf{r}_k$  given a data pattern  $\mathbf{s}$  is calculated by the circularly-asymmetric Gaussian model as follows:

$$\Pr(\mathbf{r}_k | \mathbf{s}) = \frac{1}{\sqrt{\det[2\pi\boldsymbol{\Sigma}(\mathbf{s})]}} \exp\left(-\frac{1}{2}(\mathbf{r}'_k - \boldsymbol{\mu}(\mathbf{s}))^T \boldsymbol{\Sigma}(\mathbf{s})^{-1} (\mathbf{r}'_k - \boldsymbol{\mu}(\mathbf{s}))\right). \quad (3)$$

Its log-likelihood is then expressed as

$$\ln \Pr(\mathbf{r}_k | \mathbf{s}) = -\frac{1}{2}(\mathbf{r}'_k - \boldsymbol{\mu}(\mathbf{s}))^T \boldsymbol{\Sigma}(\mathbf{s})^{-1} (\mathbf{r}'_k - \boldsymbol{\mu}(\mathbf{s})) - \frac{1}{2} \ln \det[2\pi\boldsymbol{\Sigma}(\mathbf{s})]. \quad (4)$$

Note that it reduces to a simplified function of the Euclidean distance,  $\|\mathbf{r}'_k - \boldsymbol{\mu}(\mathbf{s})\|$ , when no information of the covariance is available. The benefit of the second-order statistics is twofold: i) less-noisy samples are prioritized via diagonal variance information and ii) correlated nonlinear noise is effectively whitened via off-diagonal correlation information. The extension to the use of the third-order statistics (skewness) is rather straightforward by using the multivariate skew-normal distribution [12].

## 2.3 Statistics Updating

The empirical mean in (1) and the empirical covariance in (2) can be updated periodically or continuously with a pre-defined training sequence or a hard-decision data. To track the time-varying statistics, one can use an exponentially-weighted mean and covariance as  $\boldsymbol{\mu}(\mathbf{s}) \leftarrow \nu \boldsymbol{\mu}(\mathbf{s}) + \mathbf{r}'_j$  and  $\boldsymbol{\Sigma}(\mathbf{s}) \leftarrow \nu \boldsymbol{\Sigma}(\mathbf{s}) + (\mathbf{r}'_j - \boldsymbol{\mu}(\mathbf{s})) (\mathbf{r}'_j - \boldsymbol{\mu}(\mathbf{s}))^T$  with an appropriate normalization of  $(1 - \nu)$  where  $0 < \nu < 1$  is referred to as a forgetting factor. Note that the determinant and the inverse of the covariance matrix, those of which are required for the likelihood calculations as in (4), can be efficiently updated by the Sherman-Morrison formula [11] as follows:

$$\ln \det[\boldsymbol{\Sigma}(\mathbf{s})] \leftarrow \ln \det[\boldsymbol{\Sigma}(\mathbf{s})] + 2N \ln \nu + \ln c, \quad (5)$$

$$\boldsymbol{\Sigma}(\mathbf{s})^{-1} \leftarrow \frac{1}{\nu} \boldsymbol{\Sigma}(\mathbf{s})^{-1} - \frac{1}{c} \mathbf{b} \mathbf{b}^T, \quad (6)$$

where we define

$$\mathbf{b} \triangleq \frac{1}{\nu} \boldsymbol{\Sigma}(\mathbf{s})^{-1} (\mathbf{r}'_j - \boldsymbol{\mu}(\mathbf{s})), \quad c \triangleq 1 + \mathbf{b}^T (\mathbf{r}'_j - \boldsymbol{\mu}(\mathbf{s})). \quad (7)$$

It reduces the computational complexity from the cubic order  $\mathcal{O}[(2N)^3]$  to the square order  $\mathcal{O}[(2N)^2]$  for the matrix inversion, where  $\mathcal{O}[\cdot]$  denotes the complexity order.

## 2.4 Excess Window Size

The window size  $M$  for the transmission data  $\mathbf{s}_k$  should

be optimized to deal with the memory length of the fiber channel. However, the total number of possible patterns increases exponentially with the window size  $M$ . Hence, we may need to use a restricted window size in practice, for example  $M = 3$  taps. On the other hand, the computational complexity just increases linearly with the window size  $N$  for the receiving data  $\mathbf{r}_k$ . We propose to use an excess window size, where we can use  $N > M$  to enhance the performance. Doing so, we can keep the computational complexity low while a longer channel memory is considered with its cross correlation in  $\Sigma(\mathbf{s})$ .

## 2.5 Fractionally-Spaced Processing

Furthermore, we introduce a fractionally-spaced processing to improve the performance by exploiting the correlation over the symbol transition. Let  $P$  be an oversampling factor. The received signal sequence is stored as  $\mathbf{r}_k = [r_{kP - \lfloor (N-1)/2 \rfloor}, \dots, r_{kP}, \dots, r_{kP + \lfloor N/2 \rfloor}]^T \in \mathbb{C}^N$  in the  $N$ -sample shift register. The fractionally-spaced statistical sequence equalizer (FS-SSE) has an advantage especially when the transceiver filters have an inter-symbol interference due to the non-ideal Nyquist filtering. In addition, the symbol timing error is absorbed by oversampling.

## 2.6 Cascading with DBP

Since the proposed equalizer cannot use a large window tap size  $M$  due to the complexity issue in practice, an FDE to compensate the chromatic dispersion is useful as a pre-processing unit to shorten the effective channel memory. To shorten the channel memory more effectively, we can adopt some nonlinear compensation techniques including the DBP [3], [4] as a pre-processor. For such a cascaded use, the DBP partly inverts the fiber nonlinearity, and the residual distortion with limited memory is dealt with by the FS-SSE. As we can see later, by using a reduced-complexity DBP with a small number of steps for SSFM computations, an equalizer cascaded with DBP and FS-SSE can enjoy a significant performance improvement while the overall complexity is maintained to be reasonably low for practical applications.

Although we focus on the hard-decision MLSE equalizer in this paper, the equalizer can be readily extended to a soft-decision equalizer including a soft-output Viterbi algorithm (SOVA) and a maximum *a posteriori* (MAP) equalizer. In [13], the authors extended the proposed statistical equalizer to the MAP receiver for a turbo equalization in the system employing a soft-input soft-output decoder for forward error correction (FEC) codes.

# 3. Performance Evaluations

## 3.1 Fiber Plant Configuration

For simulations, we use the fiber link configuration corresponding to the experimental setup used in [6]. The channel

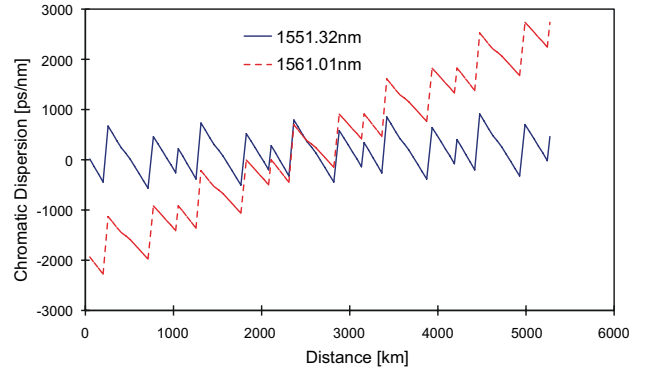


図3 光ファイバの波長分散マップ (波長 1551 nm , 1561 nm) .

Fig. 3 Fiber channel dispersion maps (wavelength: 1551 nm and 1561 nm).

is a 10 Gbaud NRZ DP-QPSK or DP-DQPSK signal with a center wavelength of 1551.32 nm or 1561.01 nm. Fig. 3 illustrates the dispersion maps of both channels, where we can see a low local dispersion for 1551 nm and high local dispersion for 1561 nm. After pre-dispersion compensation, the signal is propagated through 5 loops of 18 spans of non-zero dispersion shift fiber (NZ-DSF) and 3 spans of standard single-mode fiber (SSMF) with compensating erbium-doped fiber amplifiers (EDFAs) (5 dB noise figure), post-dispersion compensation and an optical filter (4-th order Gaussian filter with a bandwidth of  $2.5 \times 10$  GHz). Coherent detection is performed using a hybrid mixer and balanced photo-detectors. The electric transmit filter uses a 25 ps rise-time Gaussian pulse, and the receiver uses a 4-th order Bessel filter with a cutoff of 75 % of the symbol rate. After digitizing to 8 samples per symbol the residual dispersion is removed using a linear frequency-domain equalizer (FDE) and the  $P$ -times oversampled signal is fed into the statistical sequence equalizer. The fiber distance per loop is 1,046 km. The Q-factor is calculated by bit error counting. We assume no PMD in simulations, and use a circular polarization basis so that two parallel equalizers for each polarization work individually.

## 3.2 Q versus Launching Power

Figs. 4(a) and 4(b) show the simulation results of Q-factor for DP-DQPSK in low local dispersion channels (1551.32 nm wavelength) and high local dispersion channels (1561.01 nm wavelength) respectively, after 5 loops (5,230 km). Here, “1Tap” denotes a 1-tap equalizer which performs as a phase compensation filter with no memory. The notation of “3Tap” stands for the proposed fractionally-spaced statistical sequence equalizer with  $M = 3$  taps,  $N = 9$  excess window and  $P = 2$  oversampling. “DBP” denotes the DBP using manually optimized SSFM parameters. “Conv. 3Tap” denotes the conventional 3-tap statistical equalizer [10] without using the second-order statistics, excess window, and oversampling.

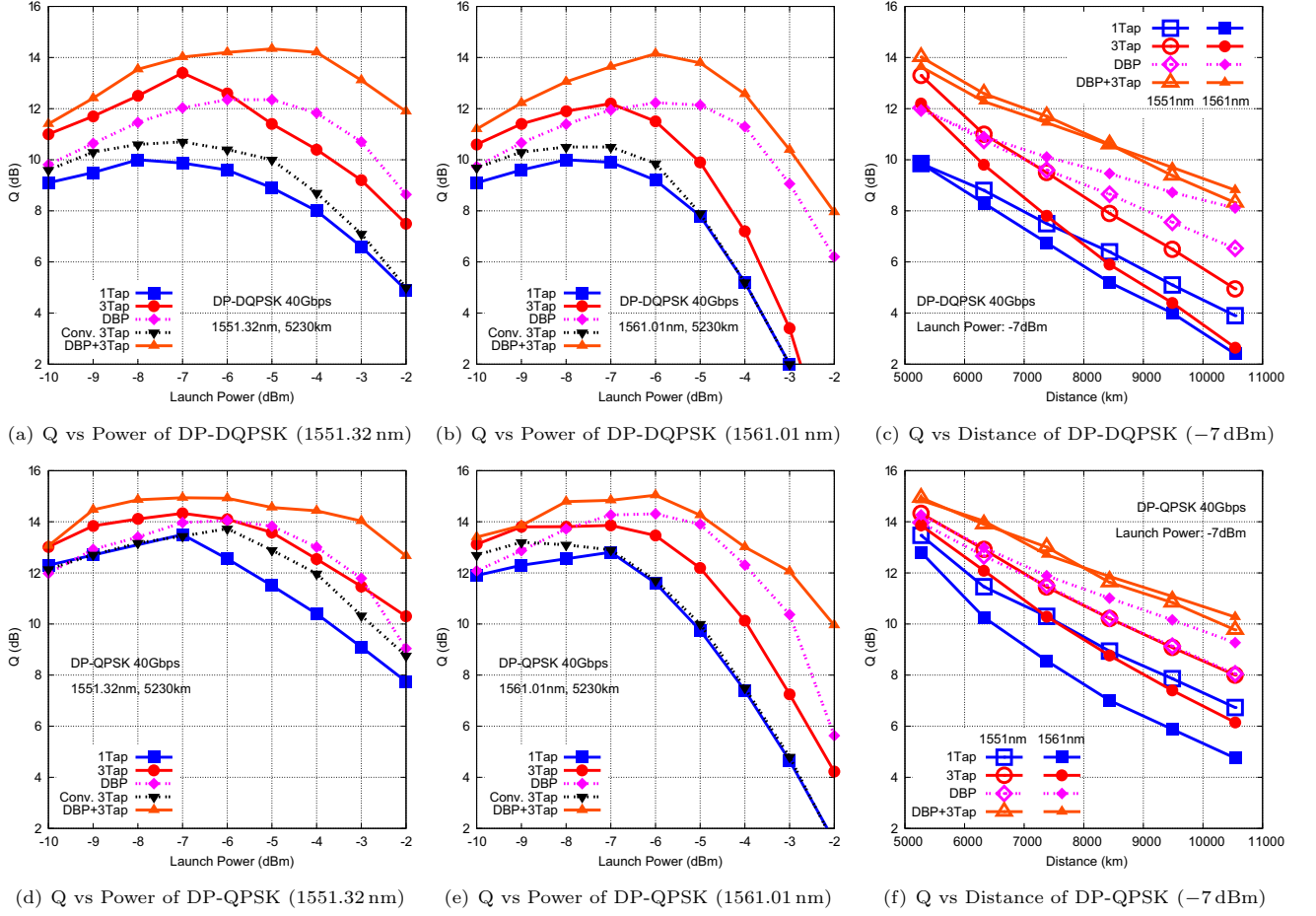


図4 送信電力・ファイバ長に対する Q ファクタ特性 ( DP-DQPSK および DP-QPSK , 40 Gbps ) .

Fig. 4 Simulation results of Q-factor performance as a function of launching power and fiber distance for 40 Gbps DP-DQPSK and DP-QPSK.

Comparing to 1-tap phase compensation method, one can see that an improvement of higher than 2 dB in Q is achieved by the proposed fractionally-spaced equalizer with 3 taps. It should be noted that such a large gain is not obtained when we use the conventional statistical equalizer [10] with such a small number of taps, since the scheme does not exploit the second-order statistics and oversampled signals. Moreover, the proposed equalizer can outperform the DBP (which uses 1 step per span, requiring 210 Fourier transform operations), in low local dispersion channels as shown in Fig. 4(a). Even for high local dispersion channels shown in Fig. 4(b), the fractionally-spaced 3-tap equalizer achieves comparable performance in peak Q factor to the DBP. More importantly, the proposed equalizer offers an additional 1–2 dBQ improvement when the DBP is used as a pre-processor. The analogous behavior is seen in Figs. 4(d) and 4(e) where DP-QPSK signals are used.

### 3.3 Q versus Fiber Distance

Figs. 4(c) and 4(f) show Q values as a function of the fiber distance for DP-DQPSK and DP-QPSK at a launching power of  $-7$  dBm, with increments of the fiber distance

further from 5,230 km to 10,460 km by 1,046 km loop each. The Q performance degrades with the fiber distance. Compared to the 1-tap equalizer, the proposed statistical sequence equalizer still obtains 1 dBQ improvement even at 10,460 km for low local dispersion case, whereas the improvement is considerably reduced for high local dispersion case. It suggests that such a small tap equalizer should work with channel shortening methods for long-haul transmissions. The DBP itself works well for long-haul transmissions. And it is observed that the cascaded equalizer using both the DBP and FS-SSE achieves the best performance; more than 4 dB gain from the 1-tap equalizer at 10,460 km. The cascaded equalizer exhibits more robust performance against the local dispersion difference in long-haul transmissions.

### 3.4 Beyond 100 Gbps Transmissions

We evaluate the performance for higher-speed data rates beyond 100 Gbps in Fig. 5, where we assume a baud rate of 28 GHz, resulting into 112 Gbps with DP-DQPSK. Since the channel memory increases as approximately 3 times large as that of the 40 Gbps case in Fig. 4, the 3-tap FS-SSE itself has no performance gain against the 1-tap equalizer. Never-

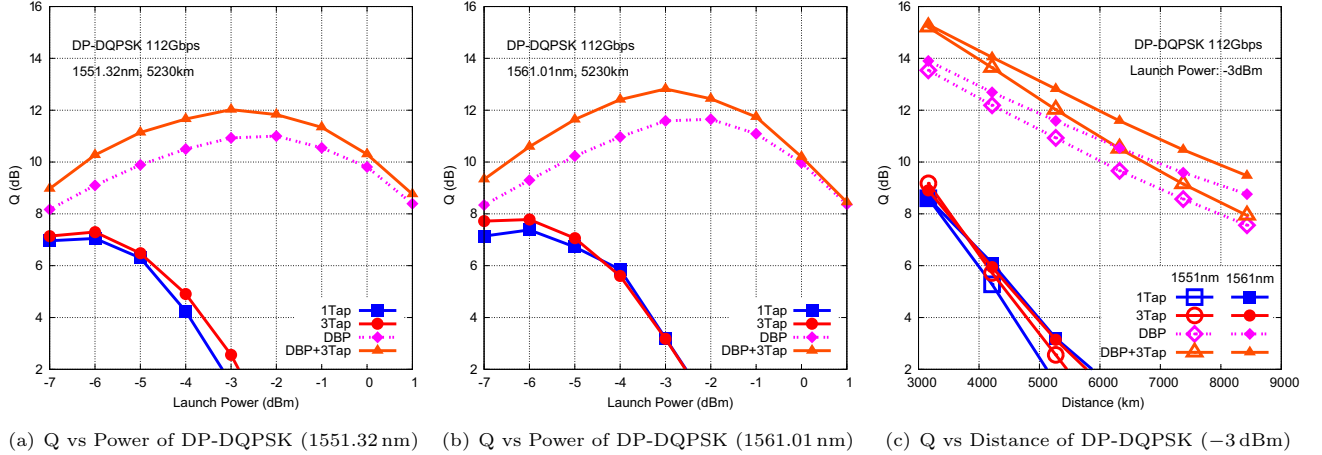


図 5 112 Gbps 高速伝送時の送信電力・ファイバ長に対する Q ファクタ特性 (DP-DQPSK) .

Fig. 5 Simulation results of Q-factor performance as a function of launching power and fiber distance for 112 Gbps high-speed DP-DQPSK.

theless, the 3-tap FS-SSE cascaded with DBP can improve the Q-factor by around 1dB compared to the DBP alone.

#### 4. Summary

We proposed the fractionally-spaced statistical sequence equalizer (FS-SSE) which exploits the second-order multivariate statistics of the fiber nonlinearity to mitigate nonlinear impairments that depend on a transmission data pattern. Through the computer simulations, a significant performance improvement of more than 2 dBQ was obtained for 40 Gbps coherent fiber-optic communication systems over 5,230 km. It was verified that oversampling with higher-order statistics can provide a significant gain compared to the existing statistical equalizer. More importantly, a short-memory equalizer with just 3 taps could achieve better performance than the DBP in low local dispersion conditions. We also demonstrated that the joint use of DBP and FS-SSE achieves an additional 1–2 dB gain due to the channel shortening effect. Even higher statistics including skewness and kurtosis can be readily introduced in the proposed method for further accurate nonlinearity modeling. The extension to the system with the inter-channel nonlinearity in wavelength-division multiplexing remains as a future work.

#### Acknowledgment

This research is in part supported by the National Institute of Information and Communication Technology (NICT) of Japan under “ $\lambda$  Reach Project.”

#### 文 献

- [1] J. Renaudier, G. Charlet, P. Tran, M. Salsi, and S. Bigo, “A performance comparison of differential and coherent detections over ultra long haul transmission of 10Gb/s BPSK,” *OFC’07, OWM1*, 2007.
- [2] A.D. Ellis, J. Zhao, and D. Cotter, “Approaching the nonlinear Shannon limit,” *JLT*, vol. 28, no. 4, pp. 423–433,

- 2010.
- [3] X. Li, X. Chen, G. Goldfarb, E. Mateo, I. Kim, F. Yaman, and G. Li, “Electronic post-compensation of WDM transmission impairments using coherent detection and digital signal processing,” *Opt. Express*, vol. 16, no. 2, pp. 880–888, 2008.
- [4] E. Ip and J.M. Kahn, “Compensation of dispersion and nonlinear impairments using digital backpropagation,” *JLT*, vol. 26, no. 20, pp. 3416–3425, 2008.
- [5] E. Ip, N. Bai, and T. Wang, “Complexity versus performance tradeoff in fiber nonlinearity compensation using frequency-shaped, multi-subband backpropagation,” *OFC’11, OThF4*, 2011.
- [6] T. Yoshida, T. Sugihara, H. Goto, T. Tokura, K. Ishida, and T. Mizuochi, “A study on statistical equalization of intra-channel fiber nonlinearity for digital coherent optical systems,” *ECOC’11, Tu.3.A.1*, 2011.
- [7] W. Yan, Z. Tao, L. Dou, L. Li, S. Oda, T. Tanimura, T. Hoshida, and J.C. Rasmussen, “Low complexity digital perturbation back-propagation,” *ECOC’11, Tu.3.A.2*, 2011.
- [8] F.P. Guiomar, J.D. Reis, A. Teixeira, and A.N. Pinto, “Mitigation of intra-channel nonlinearities using a frequency-domain Volterra series equalizer,” *ECOC’11, Tu.6.B.1*, 2011.
- [9] N. Alić, G.C. Papen, R.E. Saperstein, L.B. Milstein, and Y. Fainman, “Signal statistics and maximum likelihood sequence estimation in intensity modulated fiber optic links containing a single optical preamplifier,” *Opt. Express*, vol. 13, no. 12, pp. 4568–4579, 2005.
- [10] Y. Cai, D.G. Foursa, C.R. Davidson, J.X. Cai, O. Sinkin, M. Nissov, and A. Pilipetskii, “Experimental demonstration of coherent MAP detection for nonlinearity mitigation in long-haul transmissions,” *OFC’10, OTuE1*, 2010.
- [11] G.H. Golub and C.F. Van Loan, *Matrix Computations, 3rd Ed.*, Johns Hopkins University Press, Oct. 1996.
- [12] A. Azzalini and A. Capitanio, “Statistical applications of the multivariate skew normal distribution,” *J. Royal Statistical Society: Series B*, vol. 61, no. 3, pp. 579–602, 1999.
- [13] C. Duan, K. Parsons, T. Koike-Akino, R. Annamajjala, K. Kojima, T. Yoshida, T. Sugihara, and T. Mizuochi, “A low-complexity sliding-window turbo equalizer for nonlinearity compensation,” *to-appear in OFC’12, JW2A.59*, 2012.